

# Coulomb explosion of CS<sub>2</sub> molecule under an intense femtosecond laser field\*

Xiao Wang(王潇)<sup>1</sup>, Jian Zhang(张健)<sup>1</sup>, Shi-An Zhang(张诗按)<sup>1,2,†</sup>, and Zhen-Rong Sun(孙真荣)<sup>1</sup>

<sup>1</sup>State Key Laboratory of Precision Spectroscopy, East China Normal University, Shanghai 200062, China

<sup>2</sup>NYU-ECNU Institute of Physics at NYU Shanghai, Shanghai 200062, China

(Received 3 November 2015; revised manuscript received 16 January 2016; published online 5 April 2016)

We experimentally demonstrate the Coulomb explosion process of CS<sub>2</sub> molecule under a near-infrared (800 nm) intense femtosecond laser field by a DC-sliced ion imaging technique. We obtain the DC-sliced images of these fragment ions S<sup>+</sup>, S<sup>2+</sup>, CS<sup>+</sup>, and CS<sup>2+</sup> by breaking one C–S bond, and assign their Coulomb explosion channels by considering their kinetic energy release and angular distribution. We also numerically simulate the dissociation dynamics of parent ions CS<sub>2</sub><sup>k+</sup> ( $k = 2-4$ ) by a Coulomb potential approximation, and obtain the time evolution of Coulomb energy and kinetic energy release, which indicates that the dissociation time of parent ions CS<sub>2</sub><sup>k+</sup> decreases with the increase of the charge number  $k$ . These experimental and theoretical results can serve as a useful benchmark for those researchers who work in the related area.

**Keywords:** Coulomb explosion, molecular photodissociation, femtosecond laser field

**PACS:** 33.80.Gj, 34.20.Gj, 42.50.Hz

**DOI:** 10.1088/1674-1056/25/5/053301

## 1. Introduction

With the dramatic development of ultrashort laser technique in the past few decades, the ultrashort intense laser field has brought out some unprecedented physical phenomena, such as multi-photon ionization (MPI),<sup>[1–3]</sup> enhanced ionization (EI) or charge-resonance enhanced ionization (CERI),<sup>[4–9]</sup> above-threshold ionization (ATI),<sup>[10]</sup> dissociative ionization,<sup>[11–14]</sup> Coulomb explosion (CE),<sup>[15–23]</sup> and so on. As is well known, when the laser intensity is up to 10<sup>14</sup> W/cm<sup>2</sup>, the laser field magnitude is comparable to the Coulomb field generated by an atomic nucleus, the molecular geometry structure can be modified, and thus the molecular chemical bond will be broken by the strong Coulomb repulsive force. Several experimental results indicated that the chemical bond will be stretched from the equilibrium nuclear distance ( $R_e$ ) in the neutral molecule to a critical distance ( $R_c$ ), and the CE process occurs at this critical distance.<sup>[6,23–28]</sup> Schmidt *et al.*<sup>[29]</sup> explained this phenomenon on the basis of a laser-induced stabilization, and found that the bond elongation is mainly determined by the molecule itself. Based on this viewpoint, Corkum *et al.*<sup>[4]</sup> proposed a theoretical model of laser-induced electron localization enhanced ionization, which concluded that the ionization of the parent ion will be dramatically enhanced around the critical distance  $R_c$  since the electron can directly tunnel through the narrow internal barrier to the continuum. Similarly, Bandrauk *et al.*<sup>[5,6]</sup> presented a charge resonance enhanced ionization model, and showed that the enhanced ionization probability at the critical distance  $R_c$  is at-

tributed to the transitions between a pair of charge-resonant states that are strongly coupled to the laser field.

As a prototypical linear triatomic molecule, the photoionization and photodissociation of CO<sub>2</sub> and CS<sub>2</sub> molecules under the intense femtosecond laser fields have been extensively studied. As a representative study of the CO<sub>2</sub> molecule, Wu *et al.*<sup>[30,31]</sup> studied the three-body fragmentation dynamics of CO<sub>2</sub> molecule in intense laser fields by using a triple ion coincidence technique, and showed that the geometric structure of CO<sub>2</sub><sup>n+</sup> ( $n = 3-6$ ) before fragmentation is close to that of neutral CO<sub>2</sub>, and both the sequential and non-sequential fragment processes can occur in the parent ions CO<sub>2</sub><sup>3+</sup>, while the parent ions CO<sub>2</sub><sup>n+</sup> ( $n = 4-6$ ) can only produce the non-sequential fragment process. In the studies of the CS<sub>2</sub> molecule, Graham *et al.*<sup>[32]</sup> measured the angular distributions of those fragment ions from the CE process of parent ions, and found that the distribution of fragment ions S<sup>m+</sup> is perpendicular to that of fragment ions C<sup>n+</sup>. Mathur *et al.*<sup>[33]</sup> defined CS<sub>2</sub> molecule as the boundary between a “heavy” molecule (like I<sub>2</sub> or its derivatives) and a “light” molecule (like H<sub>2</sub> or N<sub>2</sub>), and showed that the geometric alignment mechanism dominates for the 100-fs laser pulses, while dynamic alignment occurs for the 35-ps laser pulses. Yamanouchi *et al.*<sup>[18–20]</sup> utilized a triple coincidence momentum imaging technique to study both sequential and non-sequential three-body CE processes, i.e., CS<sub>2</sub><sup>3+</sup> → S<sup>+</sup> + C<sup>+</sup> + S<sup>+</sup>, and demonstrated that the significant structural deformation occurs for CS<sub>2</sub><sup>3+</sup> along both bending and stretching coordinates. In previous studies, this coin-

\*Project supported by the National Natural Science Foundation of China (Grant Nos. 51132004 and 11474096), and the Science and Technology Commission of Shanghai Municipality, China (Grant No. 14JC1401500). We acknowledge the support of the NYU-ECNU Institute of Physics at NYU Shanghai.

†Corresponding author. E-mail: sazhang@phy.ecnu.edu.cn

cidence measurement technique can identify a specific single event of Coulomb explosion from a single parent ion, but it has relatively high requirement for the chamber vacuum pressure and sample vapor temperature. Recently, the DC-sliced ion imaging technique has shown to be a well-established tool to study the molecular photoionization and photodissociation process, where both the speed and angular distributions of the produced ions can be directly measured without any mathematical transformation, and so can provide a more intuitive method. In this paper, we experimentally investigate the CE process of  $\text{CS}_2$  molecule under an intense near-infrared (800 nm) femtosecond laser field by the DC-sliced ion imaging technique. The DC-sliced images of four ions  $\text{S}^+$ ,  $\text{S}^{2+}$ ,  $\text{CS}^+$ , and  $\text{CS}^{2+}$  by breaking one C–S bond are measured, and their Coulomb explosion channels are assigned by calculating kinetic energy release (KER) and their angular distributions are extracted from the DC-sliced images. The dissociation dynamics of parent ions  $\text{CS}_2^{k+}$  ( $k = 2, 3, 4$ ) is numerically simulated by using a Coulomb energy approximation, and it is shown that the dissociation time decreases when the charge number increases.

## 2. Experimental setup

Details of our home-built DC-sliced ion imaging system have been described in our earlier publication,<sup>[27]</sup> and only a brief description is given here. The  $\text{CS}_2$  sample (99.9% purity) carried by 1 atm helium gas is expanded adiabatically into the source chamber through a pulsed valve with the repetition rate of 100 Hz, and then skimmed into the high-vacuum main chamber with a base pressure of  $\sim 10^{-8}$  mbar. The multi-stage ion lens in the main chamber has a similar configuration described by Suits *et al.*,<sup>[34]</sup> and the optimized voltages applied on the electrodes are  $U_{\text{Repeller}} = 2000$  V,  $U_1 = 1760$  V,  $U_2 = 1660$  V, and  $U_3 = 0$  V. The super-sonic molecular beam interacts with the intense femtosecond laser field in the main chamber, and the fragment ions are first accelerated by a multi-lens velocity mapping apparatus and then fly freely to a dual micro-channel plate (MCP) coupled with a P47 phosphor screen. The sliced images of the fragment ions are obtained with an intensified charge-coupled device (ICCD) camera, and the time-of-flight (TOF) mass spectra are achieved by a photomultiplier tube (PMT) connected to a digital oscilloscope. All the timing sequence control is implemented by a digital delay pulse generator (DG535 Stanford Research System).

## 3. Results and discussion

Figure 1 shows two typical TOF mass spectra of  $\text{CS}_2$  molecule irradiated by the 800-nm femtosecond laser field with a laser central wavelength of 800 nm and the pulse duration of 70 fs for the laser intensity of  $4.9 \times 10^{13}$  W/cm<sup>2</sup>

(see Fig. 1(a)) and  $1.3 \times 10^{14}$  W/cm<sup>2</sup> (see Fig. 1(b)). In our experiment, the laser polarization direction is always perpendicular to the TOF axis. When the laser intensity is set at  $4.9 \times 10^{13}$  W/cm<sup>2</sup>, as shown in Fig. 1(a), these fragment ions  $\text{C}^+$ ,  $\text{S}^{m+}$  ( $m = 1-3$ ),  $\text{CS}^+$ ,  $\text{CS}_2^+$ , and  $\text{CS}_2^{2+}$  can be observed, which indicates that the two C–S bonds can be broken in this lower laser intensity. When the laser intensity is increased to  $1.3 \times 10^{14}$  W/cm<sup>2</sup>, as shown in Fig. 1(b), some highly charged fragment ions  $\text{C}^{2+}$ ,  $\text{C}^{3+}$  and  $\text{S}^{4+}$  appear, which shows that the appearance potential of fragment ion  $\text{C}^{m+}$  is higher than that of fragment ion  $\text{S}^{m+}$  with the same charge number. Generally, the generation of highly charged ions (such as  $\text{C}^{2+}$ ,  $\text{C}^{3+}$ ,  $\text{S}^{2+}$ ,  $\text{S}^{3+}$ ,  $\text{S}^{4+}$ ) indicates the participation of the CE processes in our experiment. In addition to the two parent ions  $\text{CS}_2^+$  and  $\text{CS}_2^{2+}$ , no other multiply charged parent ions are observed at the full range of our laser intensities, which may be due to the instability of the highly charged parent ions. In this work, we aim to explore the formation mechanism of fragment ions  $\text{S}^+$ ,  $\text{S}^{2+}$ ,  $\text{CS}^+$ , and  $\text{CS}^{2+}$  by breaking one C–S bond.

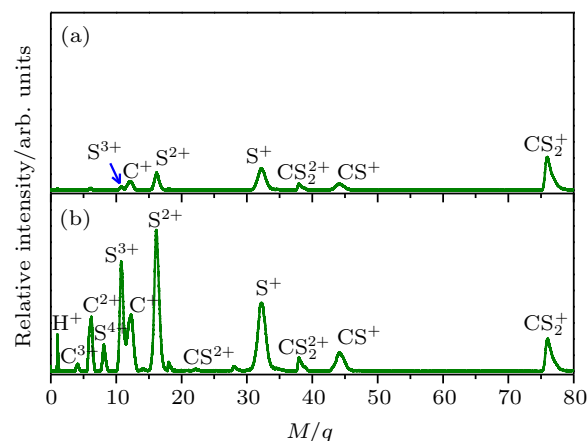


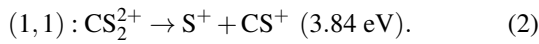
**Fig. 1.** (color online) The TOF mass spectra of  $\text{CS}_2$  molecule irradiated by 800 nm femtosecond laser pulses with a laser intensity of  $4.9 \times 10^{13}$  (a) and  $1.3 \times 10^{14}$  W/cm<sup>2</sup> (b).

When the polyatomic molecules are subjected to an intense femtosecond laser field, the fragment ions can be produced from different photoionization and photodissociation channels. With the help of DC-sliced image technique, we can clearly discriminate these different dissociative ionization channels of the fragment ions with same mass-to-charge ratio. Figure 2 presents the pseudo-color DC-sliced images of fragment ions  $\text{S}^+$ ,  $\text{S}^{2+}$ ,  $\text{CS}^+$ , and  $\text{CS}^{2+}$ . One can see that each fragment ion involves more than one dissociative ionization channel. Usually, the fragment ions with high KER should result from the CE process, while those with low KER should result from the multi-photon dissociative ionization process. Here we focus on the CE process of the four fragment ions. As is well known, in the two-body CE model, the two partner ions should meet with the momentum conservation condition. In other words, the KERs of the two fragments should satisfy

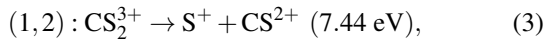
the following relationship:<sup>[27,35,36]</sup>

$$\frac{\text{KER}(X^{p+})}{\text{KER}(Y^{q+})} = \frac{M(Y^{q+})}{M(X^{p+})}, \quad (1)$$

where  $X$  and  $Y$  represent the partner fragment ions,  $M$  is the mass of corresponding fragment ions, and  $p, q$  are charge numbers of the two fragment ions. Figure 3 shows the velocity distributions of the four fragment ions  $S^+$ ,  $S^{2+}$ ,  $CS^+$ , and  $CS^{2+}$ , and the calculated kinetic energies of these different peaks are also labeled. In order to facilitate the discussion below, these peaks from low to high kinetic energy are respectively labeled with the symbols  $P_x$  ( $x = 1-3$ ). According to Eq. (1), it can be deduced that  $P_1$  peak in the fragment ion  $S^+$  and  $P_2$  peak in the fragment ion  $CS^+$  should come from the two-body CE process,



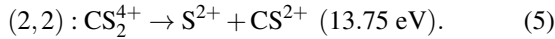
Applying the same method,  $P_3$  peak in the fragment ion  $S^+$  and  $P_2$  peak in the fragment ion  $CS^{2+}$  can be assigned to the two-body CE process,



while the  $P_1$  peak in the fragment ion  $S^{2+}$  and  $P_3$  peak in the fragment ion  $CS^+$  can be attributed to such a two-body CE process,



Similarly, the  $P_2$  peak in the fragment ion  $S^{2+}$  and  $P_3$  peak in the fragment ion  $CS^{2+}$  can be verified as the two-body CE process below,



However, we cannot find a corresponding peak in Fig. 3 to match  $P_3$  peak in fragment ion  $S^{2+}$ , whose partner ion might experience further dissociation or CE process.

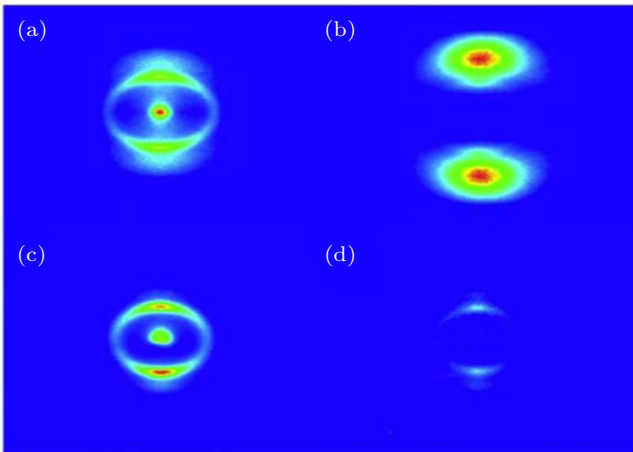


**Fig. 2.** (color online) The pseudo-color DC sliced images of fragment ions  $S^+$  (a),  $S^{2+}$  (b),  $CS^+$  (c), and  $CS^{2+}$  (d) with the laser intensity of  $1.5 \times 10^{14} \text{ W/cm}^2$ .

Table 1 lists the mass ratio  $M(CS^{q+})/M(S^{p+})$ , KER ratio  $(S^{p+})/\text{KER}(CS^{q+})$ , and relative experimental error  $\Delta$ . Considering the experimental condition and data processing, if the experimental error  $\Delta$  is less than 5%, the above listed channel assignments are considered to be correct. As can be seen, both the channels (1,2) and (2,1) result from the CE process of parent ion  $CS_2^{3+}$ , but their total KERs are different, which can come from the different precursor states. In addition, there is a spot in the central position for the fragment ions  $S^+$  and  $CS^+$ , which can be assigned to the (1,0) and (0,1) dissociative ionization channels of parent ion  $CS_2^+$ . Here, we do not discuss this dissociation process since our focus is the CE process.

**Table 1.** Mass ratio  $\frac{M(CS^{q+})}{M(S^{p+})}$  (Ratio1), KER ratio  $\frac{\text{KER}(S^{p+})}{\text{KER}(CS^{q+})}$  (Ratio2), and relative error  $\Delta = \left| \frac{\text{Ratio2} - \text{Ratio1}}{\text{Ratio1}} \right|$  for the four CE channels.

Channels	$E_{\text{total}}/\text{eV}$	$R_c/\text{\AA}$	Ratio 1	Ratio 2	$\Delta$
(1,1)	3.84	3.75	1.38	1.37	0.7%
(1,2)	7.44	3.87	1.38	1.44	4.3%
(2,1)	7.86	3.66	1.38	1.41	2.2%
(2,2)	13.75	4.19	1.38	1.33	3.6%

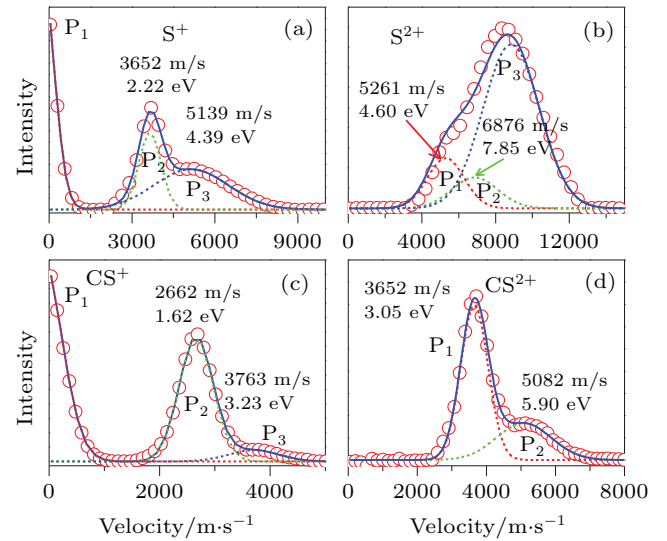


**Fig. 3.** (color online) The velocity distributions of fragment ions  $S^+$  (a),  $S^{2+}$  (b),  $CS^+$  (c), and  $CS^{2+}$  (d). The red circles are the experimental data, and the blue solid lines are the simulated results by the multiple Gaussian functions.

In addition to the KER distribution, the angular distribution of fragment ions also plays an important role in assigning the dissociation channels. The two fragment ions from the same dissociation channel should have the similar angular distribution. Figure 4 presents the angular distributions of four pairs of fragment ions mentioned above. As expected, each pair of fragment ions has a similar angular distribution, which can further verify the above CE channel assignments. Furthermore, one can see that the fragment ions that result from the dissociation process of the higher parent ions will show a narrower angular distribution.

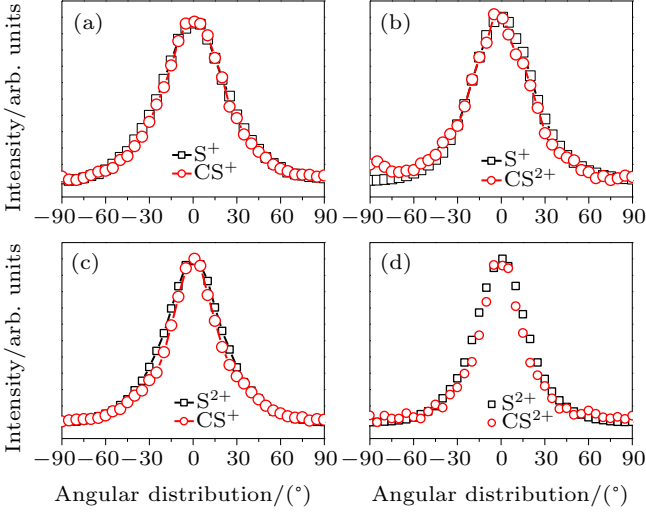


**Fig. 4.** (color online) The angular distributions of the two fragment ions that correspond to the four CE channels (1, 1) (a), (1,2) (b), (2,1) (c), and (2,2) (d).

It has been proved that the total KER  $E_{\text{total}}$  from the CE process and the critical distance  $R_c$  should satisfy the following relationship:<sup>[23,26]</sup>

$$E_{\text{total}} = 14.4 \frac{pq}{R_c}. \quad (6)$$

The calculated  $R_c$  values for the four channels are also shown in Table 1. It can be found that the chemical bond fusion in all these channels takes place at the critical distance  $R_c$  between 3.66 and 4.19 Å, which is about 2.3–2.7 times longer than the equilibrium distance of C–S bond (1.56 Å). It is noted that the bond elongation is larger for the parent ion with a larger charge number, and this phenomenon has been observed in diatomic and triatomic molecules.<sup>[37–41]</sup> The bond elongation has been explained by an enhanced ionization at a critical distance  $R_c$  where the ionization rate would be greatly enhanced, and the intense Coulomb repulsive energy will lead to the dramatic fragmentation process by converting the Coulomb energy into the KERs of the two separated fragment ions.<sup>[4–6]</sup>

To better understand this energy conversion process, we use a Coulomb potential approximation to theoretically simulate the dissociation process of parent ions, and here the doubly charged parent ion  $\text{CS}_2^{2+}$  is used as an example for detailed illustration. Assuming that the initial momentum of fragment ions  $\text{S}^+$  and  $\text{CS}^+$  are both zero, the critical distance  $R_c$  of parent ion  $\text{CS}_2^{2+}$  is known as 3.75 Å, and the two fragment ions  $\text{S}^+$  and  $\text{CS}^+$  move along the Coulomb potential. Here, we introduce the Hamiltonian in the center-of-mass coordinate system as follows:

$$H = \frac{1}{2} \sum_{i=1}^2 m_i |\dot{\mathbf{r}}_i|^2 + \frac{Ke^2}{|\mathbf{r}_{12}|}, \quad (7)$$

where  $K = 1/4\pi\epsilon_0$ , and subscript 1 and 2 represent the two fragment ions  $\text{S}^+$  and  $\text{CS}^+$ , respectively. By simplifying, equation (7) can be further written as follows:<sup>[28]</sup>

$$\ddot{x}_1 = \frac{Ke^2 m_2}{m_1(m_1 + m_2)x_1^2},$$

$$\ddot{x}_2 = -\frac{Ke^2 m_1}{m_2(m_1 + m_2)x_2^2}, \quad (8)$$

with the initial conditions,

$$x_1(0) = \frac{R_c m_2}{m_1 + m_2}, \quad x_2(0) = -\frac{R_c m_1}{m_1 + m_2},$$

$$\dot{x}_1(0) = \dot{x}_2(0) = 0.$$

In our simulation, equation (8) is solved numerically, and the time evolution of Coulomb energy and KERs in the above four channels can be obtained, as shown in Fig. 5. Obviously, the Coulomb energy dramatically decreases while KER accordingly increases for all these channels. In order to intuitively understand the energy conversion, the time requirements for different percentages of Coulomb energy to KERs in each channel are listed in Table 2. We assume that the time requirement for the energy conversion percentage of 90% is defined as the dissociation time of the parent ion,<sup>[28]</sup> which means that the C–S bond is completely broken and the parent ion  $\text{CS}_2^{k+}$  dissociates into two fragment ions  $\text{S}^{p+}$  and  $\text{CS}^{q+}$  within that time, and thus the dissociation time of these parent ions  $\text{CS}_2^{2+}$  (channel (1, 1)),  $\text{CS}_2^{3+}$  (channel (1, 2)),  $\text{CS}_2^{3+}$  (channel (2, 1)), and  $\text{CS}_2^{4+}$  (channel (2, 2)) are about 666, 498, 456, and 396 fs, respectively. It is noteworthy that the time requirement for the dissociation becomes shorter with the increase of the charge number of the parent ion. That is to say, the higher charge number will yield the stronger Coulomb repulsive force, which will accelerate the Coulomb explosion and quickly dissociate into fragmentation ions, and so the higher KER and narrower angular distribution of the fragment ions will be observed. This gives a good explanation for the experimental observation in Figs. 3 and 4 that the fragment ions with the higher KER and narrower angular distribution come from the higher parent ions. Moreover, the change tendency of the dissociation time can help us understand why no highly charged parent ions  $\text{CS}_2^{k+}$  ( $k \geq 3$ ) are observed in our experiment, as shown in Fig. 1.

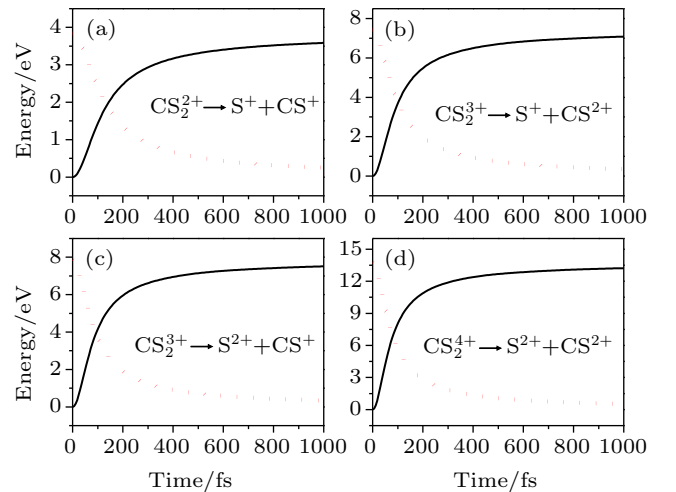


**Fig. 5.** (color online) The time evolution of Coulomb energy (red dotted lines) and KER (black solid lines) for the four CE channels  $\text{CS}_2^{2+} \rightarrow \text{S}^+ + \text{CS}^+$  (a),  $\text{CS}_2^{3+} \rightarrow \text{S}^+ + \text{CS}^{2+}$  (b),  $\text{CS}_2^{3+} \rightarrow \text{S}^{2+} + \text{CS}^+$  (c), and  $\text{CS}_2^{4+} \rightarrow \text{S}^{2+} + \text{CS}^{2+}$  (d).



**Table 2.** Time requirement for different percentages of Coulomb energy to KERs in the four CE channels.

Channels	10%	30%	50%	70%	90%
(1,1)	41	84	136	237	666
(1,2)	30	62	100	176	498
(2,1)	27	56	94	162	456
(2,2)	24	49	91	140	396

#### 4. Conclusions

In summary, the CE process of CS<sub>2</sub> molecule under the near-infrared (800 nm) intense femtosecond laser field has been experimentally investigated with a DC-sliced ion imaging technique. The CE channels of fragment ions S<sup>+</sup>, S<sup>2+</sup>, CS<sup>+</sup>, and CS<sup>2+</sup> by breaking one C–S bond were confirmed by calculating their corresponding velocity distribution and angular distribution. The Coulomb explosion process of highly charged parent ions CS<sub>2</sub><sup>k+</sup> (k = 2–4) was theoretically simulated by using a Coulomb potential approximation. It was shown that the chemical bond break occurred at a critical distance, and the dissociation time of parent ion decreased with the increase of the charge number due to the stronger Coulomb repulsive force, and the theoretical result gave a good explanation as to why the measured KER in the experiment was much smaller than the theoretical calculation and the fragment ions from the higher parent ions showed a higher KER and narrower angular distribution. We believe that these experimental and theoretical results will be very useful for further understanding the CE process of polyatomic molecule under the intense femtosecond laser field.

#### References

- [1] Vijayalakshmi K, Safvan C P, Kumar G R and Mathur D 1997 *Chem. Phys. Lett.* **270** 37
- [2] Castillejo M, Couris S, Koudoumas E and Martin M 1998 *Chem. Phys. Lett.* **289** 303
- [3] Sakai H, Stapelfeldt H, Constant E, Ivanov M Y, Matussek D R, Wright J S and Corkum P B 1998 *Phys. Rev. Lett.* **81** 2217
- [4] Seideman T, Ivanov M Y and Corkum P B 1995 *Phys. Rev. Lett.* **75** 2819
- [5] Zuo T and Bandrauk A D 1995 *Phys. Rev. A* **52** R2511
- [6] Bandrauk A D and Lu H Z 2000 *Phys. Rev. A* **62** 053406
- [7] Banerjee S, Kumar G R and Mathur D 1999 *Phys. Rev. A* **60** R25
- [8] Bryant W A, Sanderson J H, El-Zein A, Newell W R, Taday P F and Langley A J 2000 *J. Phys. B: At. Mol. Opt. Phys.* **33** 745
- [9] Sabzyan H and Vafaei M 2005 *Phys. Rev. A* **71** 063404
- [10] Agostini P, Fabre F, Mainfray G, Petite G and Rahman N K 1979 *Phys. Rev. Lett.* **42** 1127
- [11] Roeterdink W G and Janssen M H M 2002 *Phys. Chem. Chem. Phys.* **4** 601
- [12] Wang Y M, Zhang S, Wei Z R and Zhang B 2009 *Chem. Phys. Lett.* **468** 14
- [13] Rosca-Pruna F, Springate E, Offerhaus H L, Krishnamurthy M, Farid N, Nicole C and Vrakking M J J 2001 *J. Phys. B: At. Mol. Opt. Phys.* **34** 4919
- [14] Beylerian C and Cornaggia C 2004 *J. Phys. B: At. Mol. Opt. Phys.* **37** L259
- [15] Cornaggia C, Schmidt M and Normand D 1994 *J. Phys. B: At. Mol. Opt. Phys.* **27** L123
- [16] Wright J S, DiLabio G A, Matussek D R, Corkum P B, Ivanov M Y, Ellert C, Buenker R J, Alekseyev A B and Hirsch G 1999 *Phys. Rev. A* **59** 4512
- [17] Tzallas P, Kosmidis C, Philis J G, Ledingham K W D, McCanny T, Singhal R P, Hankin S M, Taday P F and Langley A J 2001 *Chem. Phys. Lett.* **343** 91
- [18] Hasegawa H, Hishikawa A and Yamanouchi K 2001 *Chem. Phys. Lett.* **349** 57
- [19] Hishikawa A, Hasegawa H and Yamanouchi K 2002 *Chem. Phys. Lett.* **361** 245
- [20] Hishikawa A, Hasegawa H and Yamanouchi K 2004 *Chem. Phys. Lett.* **388** 1
- [21] Sun S Z, Yang Y, Zhang J, Wu H, Chen Y T, Zhang S A, Jia T Q, Wang Z G and Sun Z R 2013 *Chem. Phys. Lett.* **581** 16
- [22] Wu H, Yang Y, Sun S Z, Zhang J, Deng L, Zhang S A, Jia T Q, Wang Z G and Sun Z R 2014 *Chem. Phys. Lett.* **607** 70
- [23] Zhang J, Zhang S A, Yang Y, Sun S Z, Li J, Chen Y T, Jia T Q, Wang Z G, Kong F A and Sun Z R 2014 *Phys. Rev. A* **90** 053428
- [24] Constant E, Stapelfeldt H and Corkum P B 1996 *Phys. Rev. Lett.* **76** 4140
- [25] Bandrauk A D, Musaev D G and Morokuma K 1999 *Phys. Rev. A* **59** 4309
- [26] Wang C, Ding D, Okunishi M, Wang Z G, Liu X J, Prümper G and Ueda K 2010 *Chem. Phys. Lett.* **496** 32
- [27] Yang Y, Fan L L, Sun S Z, Zhang J, Chen Y T, Zhang S A, Jia T Q and Sun Z R 2011 *J. Chem. Phys.* **135** 064303
- [28] Wu C, Zhang G Q, Wu C Y, Yang Y D, Liu X R, Deng Y K, Liu H, Liu Y Q and Gong Q H 2012 *Phys. Rev. A* **85** 063407
- [29] Schmidt M, Normand D and Cornaggia C 1994 *Phys. Rev. A* **50** 5037
- [30] Wu C, Wu C Y, Song D, Su H M, Yang Y D, Wu Z F, Liu X R, Liu H, Li M, Deng Y K, Liu Y Q, Peng L Y, Jiang H B and Gong Q H 2013 *Phys. Rev. Lett.* **110** 103601
- [31] Wu C Y, Wu C, Fan Y M, Xie X G, Wang P, Deng Y K, Liu Y Q and Gong Q H 2015 *J. Chem. Phys.* **142** 124303
- [32] Graham P, Ledingham K W D, Singhal R P, McCanny T, Hankin S M, Fang X, Smith D J, Kosmidis C, Tzallas P, Langley A J and Taday P F 1999 *J. Phys. B: At. Mol. Opt. Phys.* **32** 5557
- [33] Banerjee S, Kumar G R and Mathur D 1999 *Phys. Rev. A* **60** R3369
- [34] Guo C, Li M, Nibarger J P and Gibson G N 1998 *Phys. Rev. A* **58** R4271
- [35] Wang Y M, Zhang S, Wei Z R and Zhang B 2008 *J. Phys. Chem. A* **112** 3846
- [36] Corrales M E, Gitzinger G, Vazquez J G, Lorient V, Nalda R and Banares L 2012 *J. Phys. Chem. A* **116** 2669
- [37] Posthumus J H, Giles A J, Thompson M R and Codling K 1996 *J. Phys. B: At. Mol. Opt. Phys.* **29** 5811
- [38] Iwamae A, Hishikawa A and Yamanouchi K 2000 *J. Phys. B: At. Mol. Opt. Phys.* **33** 223
- [39] Hishikawa A, Iwamae A and Yamanouchi K 1999 *Phys. Rev. Lett.* **83** 1127
- [40] Hishikawa A, Iwamae A and Yamanouchi K 1999 *J. Chem. Phys.* **111** 8871
- [41] Iwasaki A, Hishikawa A and Yamanouchi K 2001 *Chem. Phys. Lett.* **346** 379